POLITECNICO DI TORINO
Repository ISTITUZIONALE

Combined use of cptu-sdmt and geophysical test to assess liquefaction: case studies in Emilia-Romagna (Italy)

Original
Combined use of cptu-sdmt and geophysical test to assess liquefaction: case studies in Emilia-Romagna (Italy) / Amoroso, S., Comina, C., Minarelli, L., Rollins, K., Bignardi, S., Vagnon, F., Di Buccio, F.. - ELETTRONICO. - Innovation in DMT & SDMT testing:(2024). (7th International Conference on Geotechnical and Geophysical Site Characterization Barcelona 18-21 giugno 2024) [10.23967/isc.2024.216].

Availability:
This version is available at: 11583/2991743 since: 2024-08-17T16:25:24Z

Publisher:
Scipedia

Published
DOI:10.23967/isc.2024.216

Terms of use:

This article is made available under terms and conditions as specified in the corresponding bibliographic description in the repository

Publisher copyright

(Article begins on next page)

15 November 2026

Proceedings of the 7th International Conference on Geotechnical and Geophysical Site Characterization
Barcelona, 18 - 21 June 2024

Combined use of CPTU-SDMT and geophysical test to assess liquefaction: case studies in Emilia-Romagna (Italy)

Sara Amoroso[1,2#], *Cesare* Comina[3], *Luca* Minarelli[2], *Kyle M.* Rollins[4], *Samuel* Bignardi[1], *Federico* Vagnon[5] and *Francesco* Di Buccio[1]

[1]*University of Chieti-Pescara, Department of Engineering and Geology, Viale Pindaro 42, 65129 Pescara, Italy*
[2]*Istituto Nazionale di Geofisica e Vulcanologia, Roma1 Section, Viale Crispi 43, 67100 L'Aquila, Italy*
[3]*University of Turin, Department of Earth Sciences, Via Valperga Caluso 35, 10125 Turin, Italy*
[4]*Brigham Young University, Department of Civil and Environmental Engineering, 430 Engineering Building, 84602 Provo, Utah*
[5]*Politecnico di Torino, Department of Environment, Land and Infrastructure Engineering, Corso Duca degli Abruzzi 24, 10129 Turin, Italy*
[#]*Corresponding author: sara.amoroso@unich.it*

ABSTRACT

The presence of a non-liquefiable crust overlying a liquefiable layer plays a significant role in determining the occurrence of liquefaction damage, as originally formulated by Ishihara in 1985. Following the 2010-2011 Canterbury seismic sequence (New Zealand), almost no foundation deformation occurred in areas characterized by soils susceptible to liquefaction overlaid by at least 3 m-thick intact crust. In contrast, the 2012 Emilia-Romagna earthquake (Italy) provided evidence of liquefaction in silty-sandy layers below 3 to 9 m-thick crusts. Therefore, Ishihara's approach and the variety of liquefaction severity indices need to be further tested to assess to what extent they can be considered reliable predictors of performance. This study aims at better understanding the role of non-liquefiable crusts in preventing damage to buildings and infrastructures. In this respect, in situ and laboratory tests were conducted at selected sites in Emilia-Romagna. The results of two case studies in Mirandola (Modena, Italy), which share similar soil profiles but exhibited different liquefaction evidences following the 2012 seismic sequence, are presented. Comprehensive geotechnical and geophysical surveys were performed at both the sites, by means of piezocone tests, seismic dilatometer tests, boreholes, laboratory tests, electrical resistivity tomography and multichannel analysis of surface waves. These surveys document the geotechnical and geophysical properties of the 5 m-thick non-liquefied (or potentially non-liquefiable) crust and of the liquefied (or potentially liquefiable) silty-sandy deposits. This effort is aimed at understanding how the surface layer properties contributed to the different behavior observed at the two sites during the earthquake events.

Keywords: liquefaction assessment; piezocone test; seismic dilatometer test; geophysical surveys.

1. Introduction

The presence of a non-liquefiable crust overlying a liquefiable layer has been observed to have a significant effect on sand ejecta and liquefaction damage, as originally formulated by Ishihara (1985). Later, following the 2011 Tohoku earthquake (Japan), Towhata et al. (2016) have developed a new chart to weight the liquefaction potential index (LPI) as a function of the thickness of the non-liquefiable crust (H_1). More recently, Maurer et al. (2015) and Upadhyaya et al. (2022) have also calibrated new liquefaction severity indices to introduce the influence of H_1, namely the Ishihara inspired LPI (LPI_{ish}) and the Ishihara inspired Liquefaction Severity Number (LSN_{ish}), using the dataset related to the 2010-2011 Canterbury earthquake sequence (CES, New Zealand).

Following the CES, almost no foundation deformation occurred in areas characterized by soils susceptible to liquefaction overlaid by at least 3 m-thick intact crust (van Ballegooy et al. 2014). In contrast, the 2012 Emilia-Romagna earthquake (Italy) provided evidence of liquefaction in silty-sandy layers below 3 to 9 m-thick crusts (Minarelli et al. 2022).

This study illustrates the results of a comprehensive campaign of geotechnical and geophysical surveys performed at two case studies in Mirandola (Modena, Italy), which share similar soil profiles ($H_1 \approx 5$ m) but exhibited different liquefaction evidences following the 2012 seismic sequence.

2. Geological setting

The two research sites, "Mirandola Via per Concordia" and "Mirandola Cividale" (Figure 1), belong to a wider study over the same area that investigated site effects induced by the 2012 Emilia-Romagna earthquake. In the following we will refer to these selected sites simply as "Site 7" and "Site 8", respectively. These sites are of particular interest because, despite the almost identical settings, one showed heavy liquefaction evidences while the other remained unaffected, at least to a visual investigation.

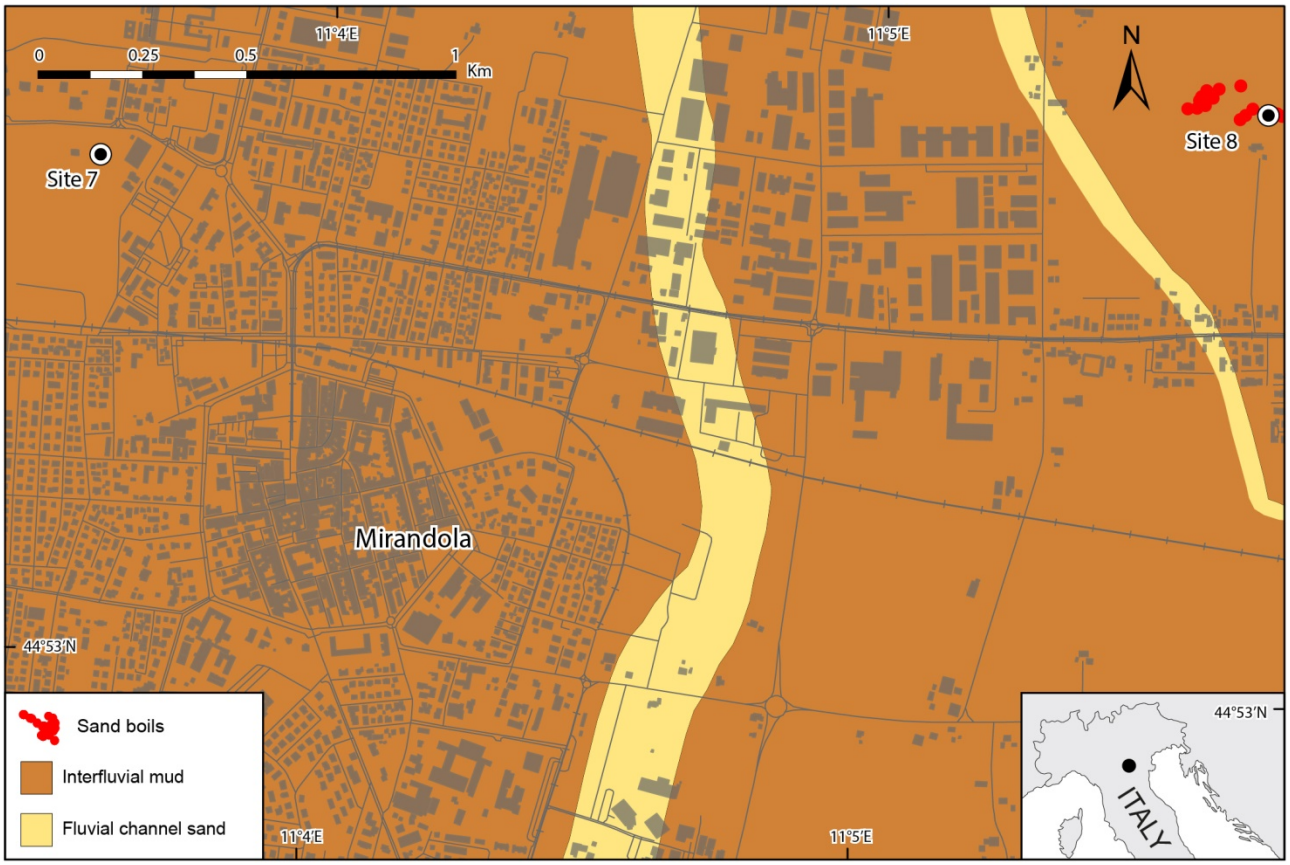


Figure 1. Engineering geological map of the outcropping alluvial deposits of the studied area Mirandola within the Emilia plain, with evidence of the liquefaction phenomena referable to the Emilia seismic sequence in 2012 (red dots).

The sites are located in the northern outskirts of the town of Mirandola (Modena, Italy) in the epicentral area of 2012 earthquake which belongs to the lower portion of the Po river alluvial plain, corresponding to the foredeep basin of the Northern Apennines chain.

The study sites are placed just north of the culmination of a ramp anticline related to the active external thrust belt of the buried Apennines Chain (Pieri and Groppi 1981). These slow-moving, yet active tectonic structures generated the 2012 May 29th main shock that triggered the liquefaction events in the Mirandola area. In the context of a wider site-effects investigation, our attention was drawn to the fact that despite of strikingly similar conditions, some locations showed very strong seismic-induced soil liquefaction, while other areas remained unaffected. We therefore decided to investigate the liquefied site in Mirandola Cividale (Site 8) and the "twin" non-liquefied site in Mirandola Via per Concordia (Site 7).

The scattered outcropping fluvial sands bodies were deposited by the Secchia river during the late Holocene, surrounded by argillaceous fluvial mud (Figure 1). In the subsurface fluvial sands abundantly form extensive coalescent bodies mainly accumulated by the Po river, during earlier Holocene times, at different depth. The base of the Holocene sands body is generally in direct erosive contact with the late Pleistocene synglacial coarse grained sands deposited by braided Po river channel.

3. Site investigation

A comprehensive geotechnical and geophysical campaign was performed at both research sites, and comprised: piezocone tests (CPTU), seismic dilatometer tests (SDMT), boreholes (S), laboratory tests, electrical resistivity tomography (ERT) and multichannel analysis of surface waves (MASW), as indicated in Figure 2.

CPTUs and SDMTs were carried out according to the international standard, using a 20 ton light penetrometer and reaching 20 m depth. At Site 8 the soundings were carried out in correspondence of the 2012 liquefied manifestations. Pore pressure readings were available both from CPTU data via the pore water pressure (u_2) and from SDMT data via the third corrected-pressure reading (p_2) allowing to detect an univocal ground water level (GWT). The SDMT test also provided a measure of the shear wave velocity (V_S), every 0.5 m depth increment.

Boreholes reached 5 m depth since they were realized using a 20 ton light penetrometer. However, disturbed samples were collected for grain-size analyses and Atterberg limits to characterize the non-liquefied (or potentially non-liquefiable) crust.

Both seismic and geoelectric geophysical tests were executed in the two test-sites along specific, and coincident, survey lines (Figure 2). All such surveys were executed in the same time period (June 2021) at both investigated sites.

Concerning the seismic tests, an array of 72, 4.5 Hz vertical geophones, at 1 m spacing for Site 7 and 1.5 m spacing for Site 8, connected to a Geometrics Geode acquisition system were used. An 8 Kg sledgehammer hit



Figure 2. Details of the studied sites and executed geotechnical and geophysical tests: (a) Site 7 – Mirandola Via per Concordia; (b) Site 8 – Mirandola Cividale. Red dots refer to the liquefaction evidences related to the 2012 May 29th main shock.

on a metallic plate was used as seismic source. The hammer was connected to the Geode with an electric trigger system. Shots where performed at 4 m offset outside the seismic line and at every 3 geophones inside the seismic line. To enhance the signal-to-noise ratio, data from 5 shots repeated at each location were averaged. Seismic data were leveraged to obtain the subsurface distribution of compressional (V_P) and shear (V_S) wave velocities. In order to obtain V_P, we picked the P-wave's first arrival times of each shot and we used the tomographic reconstruction offered by the software Rayfract (© Intelligent Resources Inc.) to obtain a 2D section of the compressional velocity. Concerning V_S, we performed both 1D and 2D Multichannel Analysis of Surface Waves (MASW) inversions. The 1D MASW inversion leveraged the sources outside the geophones line and were performed using the code SWAT (Surface Wave Analysis Tool), developed in Matlab® by the group of Applied Geophysics Laboratory of the Department Georesources of the Polytechnic of Turin. The code extracts the dispersion information from the seismogram using a frequency-wavenumber transform. Subsequently, a dispersion curve is picked and used to define an objective misfit function to be minimized during the inversion. The latter is achieved by a global search of the parameters space featuring a Monte Carlo algorithm (Socco and Boiero 2008). The global search efficiently explores a wide portion of the parameter's space ensuring that possible non-uniqueness of the solution is properly handled. The 2D inversion was achieved by leveraging the MASW dispersion curves extraction work-flow applied to consecutive 24-receivers subsets from the original 71, effectively capturing lateral changes in the dispersive behavior of surface waves. Dispersion images for each seismogram were obtained using Park's phase-shift approach (Park et al. 1998) implemented in Matlab® . These were then directly transformed in V_S profiles by means of a specific W/D procedure (e.g. Comina et al. 2020). For the geoelectric tests we employed an array of 72 stainless steel electrodes, placed at 1 m spacing for Site 7 and 1.5 m spacing for Site 8, and connected to a Syscal Pro resistivity meter (©Iris Instruments). Apparent Electric resistivity data were obtained from a total of 1287 measured values of potential. The latter acquired using the a Wenner-Schlumberger quadrupole protocol Inversion was performed leveraging the software Res2DInv (©Geotomo Software), which produces a 2D profile mapping the 2D subsurface soil resistivity.

4. Results

4.1. In situ tests

The results from the CPTU tests are summarized in Figure 3, which shows a comparison of the two sites in terms of soil behaviour type index (I_c), corrected cone penetration resistance (q_t) and sleeve friction (f_s), while Figure 4 reports the DMT profiles of the material index (I_D), horizontal stress index (K_D) and constrained modulus (M). As it can be observed, the two sites appear very similar in the soil stratigraphy identifying a silty crust of approximately 5 m in thickness, followed by a silty-sandy deposit. According to the "simplified procedure" (Seed and Idriss 1971), applied using Idriss and Boulanger (2008) CPT-method with a GWT = 3.6 m and the 2012 seismic input (moment magnitude M_W = 5.9 and peak ground acceleration PGA = 0.4g), it was possible to estimate the thickness of the non-liquefiable crust (H_1) and of the liquefiable deposit (H_2) at the two sites: $H_1 \approx 4.9$ m, characterized by a plasticity index PI $\leq$ 10%, and $H_2 \approx 1.1$ m at Site 7 (true negative point in the Ishihara 1985 chart), and $H_1 \approx 4.5$ m, characterized by PI $\leq$ 25%, and $H_2 \approx 1.5$ m at Site 8 (false negative point in the Ishihara 1985 chart). However, other interbedded liquefiable layers are detectable mainly up to 12 m for Site 7 and up to 20 m for Site 8. The in-situ geotechnical parameters in Figures 3 and 4, highlight lower values of q_t, K_D and M in the crust of the 2012 liquefied site (Site 8) when compared with the H_1 parameters of the 2012

non-liquefied site (Site 7). Similarly, q_t, K_D and M values related to H_2 found at Site 8 appears to be lower than the corresponding values obtained at Site 7. However, by looking at the silty sandy layer between 6 and 13 m the q_t, K_D and M profiles result generally higher at Site 8 than at Site 7.

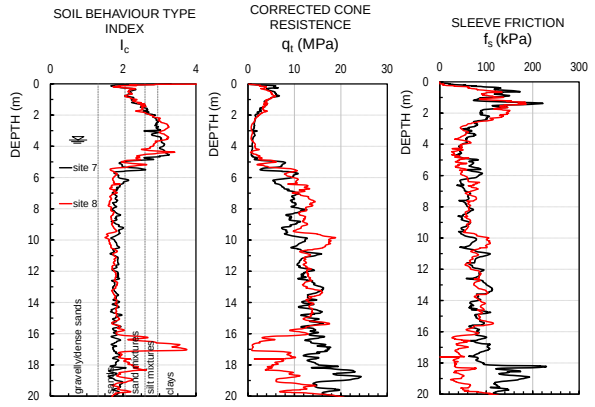


Figure 3. Results of CPTU test (black and red lines correspond to Site 7 and 8 respectively): soil behaviour type index (I_c), corrected cone penetration resistance (q_t) and sleeve friction (f_s).

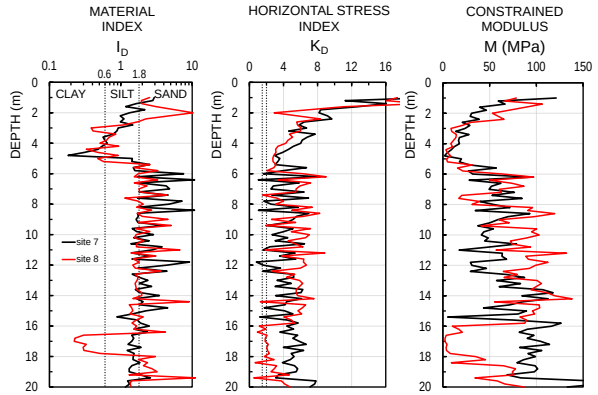


Figure 4. Results of DMT test (black and red lines correspond to Site 7 and 8 respectively): material index (I_D), horizontal stress index (K_D) and constrained modulus (M).

4.2. Geophysical surveys

In Figure 5 we compare the vertical profiles of physical properties obtained from different geophysical tests. For those surveys which output is typically a 2D section, we extracted information from underneath the position of the profile that is nearest to the location of the geotechnical tests reported in the previous section. However, it must be said that most of the 2D surveys turned out to be quite laterally homogeneous exibiting negligible lateral variations. It is worthy of note that inversion of V_S returned very similar profiles, regardless of the methodology employed (MASW1, MASW2 and SDMT), the only exception being a slightly lower Vs in some portions of Site 8. Conversely, significant differences are observed between both V_P and resistivity results of the sites. In particular, V_P of the shallow portion of the profile obtained for Site 7 is comparatively lower than that of Site 8. Both V_P profiles show a progressive increase of V_P with depth reaching the value of 1500 m/s, corresponding to full saturation, at a depth of about 8 to 10 m. This imaged depth is not in agreement with the measured water table depth at both sites (around 3.6 m). The difference in the results could be potentially related to the presence of partially saturated (even with very high water content) portions of the shallower layers. Also resistivity data show remarkable differences between the two sites. Particularly, a very low resistivity crust is depicted at Site 8 with an underlying higher resistivity sandy layer. Conversely, at Site 7 the resistivity distribution appears to be relatively homogeneous between upper crust and underlying sands.

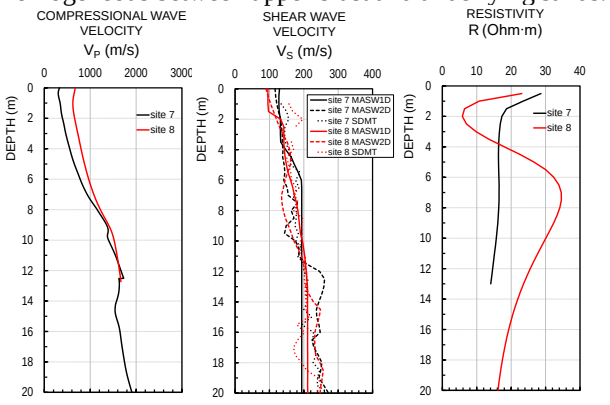


Figure 5. Results of the geophysical surveys (black and red lines correspond to Site 7 and 8 respectively): compression wave velocity (V_P), shear wave velocity (V_S) and resistivity (R).

5. Discussion

Aiming to a better understanding of the nature of non-liquefiable crusts and of the liquefiable deposits, average values of H_1 and H_2 were computed in Table 1. For the coarse-grained layer of H_2 the average parameters were calculated using the full H_2 thickness at Site 7 ($H_2 \approx 4.9$-6 m) and Site 8 ($H_2 \approx 4.5$-6 m), filtering for data for $I_c \leq 2.6$ and $I_D \geq 1.2$. Instead, for the fine-grained layer of H_1 the upper ≈ 2 m-depth layers were removed considering the high values probably due to the seasonal variations in water content caused by the GWT fluctuation, filtering for data for $I_c > 2.6$ and $I_D < 2.6$. Relative density (D_R) and friction angle (φ') in sandy deposits ($I_c \leq 2.6$), and hydraulic conductivity (K) were estimated from CPTU according to Jamiolkowski et al. (2001), Jefferies and Been (2006) and Robertson (2015), respectively. Overconsolidation ratio (OCR), in-situ earth pressure coefficient (K_0) and undrained shear strength (s_u) in fine-grained soils ($I_D < 1.2$) were evaluated from DMT proposed by Marchetti (1980). OCR and K_0 were also assessed in sandy deposits ($I_c \leq 2.6$ and $I_D \geq 1.8$) using coupled DMT-CPTU surveys in agreement with Monaco et al. (2010) and Hossain and Andrus (2016), respectively.

The comparison of the average geotechnical parameters of the non-liquefiable crust (H_1) shows that the values of q_t, k, K_D, OCR, K_0, M and s_u, found at Site 8 (2012 liquefied site) are lower than those encountered at Site 7 (2012 non-liquefied site). This aspect may be explained in relation to the changes inferred in soil structure caused by large strain destructuration of the soil mass following the liquefaction phenomena evidenced at Site 8 (e.g. Amoroso et al. 2017, Passeri et al. 2018). Higher values of hydraulic conductivity at Site 7 compared to Site 8 may also have facilitated the dissipation of the pore water pressure during the 2012

Table 1. Average geotechnical and geophysical parameters for H_1 and H_2.

		CPT					DMT or DMT+CPT						Geophysical surveys		
	Site	I_c (-)	q_t (MPa)	D_R (%)	φ' (°)	K (m/s)	I_D (-)	K_D (-)	OCR (-)	K_0 (-)	M (MPa)	s_u (kPa)	V_S (m/s)	V_P (m/s)	R (Ohm·m)
H_1	7	2.93	1.36	-	-	2.40E-08	0.55	5.33	4.76	1.20	13.42	48.85	144	491	17
	8	2.99	1.26	-	-	1.98E-08	0.62	4.42	3.52	1.05	10.16	38.19	151	742	13
H_2	7	2.01	7.45	49.26	37.50	1.34E-05	2.68	3.69	1.15	0.46	30.41	-	167	710	16
	8	2.05	5.91	39.44	37.36	2.11E-05	2.29	3.58	1.20	0.48	33.22	-	156	900	30

Table 2. Liquefaction severity indices applying or not partial saturation correction.

		No PSF correction				PSF-V_P correction				PSF-V_P/V_S correction			
Severity index	Site	CPT	DMT	DMT & CPT	V_S	CPT	DMT	DMT & CPT	V_S	CPT	DMT	DMT & CPT	V_S
LPI	7	4.38	16.17	9.77	8.13	2.31	14.22	7.40	6.38	4.34	16.14	9.73	8.09
	8	4.30	9.44	5.37	8.65	3.10	8.53	4.29	6.06	4.27	9.42	5.35	8.59
LPI_{ISH}	7	0.34	6.93	2.04	0.00	0.00	5.97	1.09	0.00	0.34	6.92	1.87	0.00
	8	1.94	5.42	1.76	1.33	1.00	4.44	1.33	0.38	1.94	5.42	1.76	1.33
LSN	7	10.39	15.56	11.14	10.50	7.97	14.21	9.11	9.20	10.34	15.56	11.04	10.50
	8	13.75	11.17	8.52	14.13	12.11	10.67	7.15	12.71	13.72	11.16	8.52	14.13
LSN_{ISH}	7	2.71	8.04	5.71	3.38	1.75	6.78	2.94	2.54	2.69	8.04	5.71	3.38
	8	6.10	5.96	4.03	5.26	5.65	5.91	3.53	3.83	6.06	5.96	4.03	5.26
S (cm)	7	8.67	14.78	11.77	10.21	6.77	13.53	10.01	9.05	8.63	14.78	11.65	10.21
	8	14.07	12.89	11.70	15.75	12.56	12.35	10.46	14.51	14.03	12.87	11.63	15.75
I_{AM}	7	0.15	0.17	0.18	0.07	0.10	0.17	0.17	0.04	0.15	0.17	0.18	0.07
	8	0.25	0.12	0.13	0.18	0.23	0.12	0.12	0.18	0.25	0.12	0.13	0.18

seismic event. In contrast, V_P values at Site 8 are higher than those observed at Site 7, therefore suggesting a higher degree of saturation (and therefore a lower cyclic resistance towards liquefaction) at Site 8 with respect to Site 7 (e.g. Tsukamoto et al. 2002). Regarding resistivity, the trend and average values mirror those of measured hydraulic conductivity with a lower resistivity in Site 8 (more electrically conductive and less permeable) with respect to Site 7.

The comparison of the average parameters of the liquefiable deposits (H_2) shows lower values of q_t, D_R, K_D, V_S and R at Site 7 (2012 non-liquefied site) compared to those at Site 8 (2012 liquefied site). Vice versa, V_P measurements are found to be higher at Site 8 than at Site 7. The differences in resistivity values may be related to different electrical conductivity of the aquifer water or local geological features of the deposit. However, a generally higher resistivity is observed in Site 8 with respect to Site 7, reflecting a stronger contrast with the overlaying crust. The increase in resistivity could be related to the presence of more compacted sands (particularly in the 6 to 10 m depth range), possibly, as a consequence of the liquefaction events. In the same depth range the resistivity results appear to be coherent with the higher q_t values evidenced from CPTU

All these aspects are in good agreement with the 2012 liquefaction observations.

Finally, Table 2 reports the following liquefaction severity indices obtained from CPTU (Idriss and Boulanger 2008), DMT (Marchetti 2016), coupled DMT and CPTU (Marchetti 2016) and V_S measurements (Andrus and Stokoe 2000): liquefaction potential index (LPI, Iwasaki et al. 1978), Ishihara inspired LPI (LPI_{ish}, Maurer et al. 2015), Liquefaction Severity Number (LSN, Tonkin and Taylor 2013), Ishihara inspired LSN (LSN_{ish}, Upadhyaya et al. 2022), liquefaction induced settlement (S, Zhang et al. 2002) and Induced dAmage Measurement (I_{AM}, Di Ludovico et al. 2020). For DMT and V_S methods the estimation of LSN, LSN_{ish}, S and I_{AM} was made possible by associating the equivalent clean sand normalized tip resistance $(q_{c1N})_{cs}$ from CPTU with the liquefaction safety factor (FS_{liq}) from DMT and V_S methods. In order to understand the influence of the partial saturation on the cyclic resistance towards liquefaction, the severity indices were also compute during the partial saturation correction factors (PSF) proposed by Tsukamoto et al. (2002) using V_P-only or V_P/V_S (Table 2).

The indices obtained without the PSF correction show a general overestimation of the liquefaction damage in comparison with the 2012 observations at Site 7. Few exceptions are related to the CPTU predictions, and for all the methods to LSN_{ish}. Vice versa, the liquefaction severity indices are in agreement with the 2012 liquefaction manifestations at Site 8 except for CPTU assessments, and for all the methods to LSN and I_{AM}. The severity indices calculated with the PSF-V_P/V_S correction do not changes significantly the numerical values of the indices calculated without correction. In contrast, some reduction of the indices is observed once the PSF-V_P correction is applied. However, this does not directly imply any overall improvement between the predictive liquefaction indices and the 2012 observations.

6. Conclusions

This study investigated two research sites in Mirandola (Italy) and aimed at understanding how the surface layer properties may contribute to the different behavior observed during the 2012 Emilia-Romagna earthquake (Italy). Geotechnical and geophysical surveys were performed at both the liquefied and non-liquefied sites, by means of CPTU, SDMT, boreholes, laboratory tests, ERT and MASW, to provide a comprehensive subsoil characterization.

The two sites featured similar soil profiles with 4.5-4.9 m-thick non-liquefied (or potentially non-liquefiable) crust and 1.5-1.1 m-thick liquefied (or potentially liquefiable) silty-sandy deposits. The geotechnical properties, obtained from CPTU and DMT, generally showed, both for H_1 and H_2, lower values at the liquefied site (Site 8 – Mirandola Cividale) than the non-liquefied site (Site 7 – Mirandola Via per Concordia), probably due to the tendency for liquefaction-induced cracking and the rise of the liquefied silty sand and sandy silt towards the surface. Conversely, the compression wave velocity resulted lower at Site 7 than at Site 8, consolidating the hypothesis of a lower degree of saturation, and therefore of a higher cyclic resistance towards liquefaction at Site 7 than at Site 8. These results were found in agreement with the 2012 observations.

The prediction of the available liquefaction severity indices only partially agrees with the field evidences from the 2012 seismic event. In particular, while an overall agreement of the index estimates and such evidence was observed for Site 8, at Site 7 we obtained in contrast a general overestimation of the liquefaction damage (absence of liquefaction) . LSN and I_{AM} indices returned unreliable results, although the latter index (I_{AM}) was calibrated using the Emilia-Romagna deposits as reference.

Further research is required to fully understand the mechanics of the non-liquefiable crusts and of the liquefiable deposits. To do so, future work will focus on extending the analysis to additional case studies and seek ways to improve the liquefaction severity index to better agree with recorded earthquake observations.

Acknowledgements

This work is partly funded by Search for Excellence – UdA 2019 (University of Chieti-Pescara, Italy), Evaluation and Improvement of Methods to Consider Influence of Surface Clay Layers on Liquefaction-Induced Settlement (CLIQUEST). However, the opinions, conclusions, and recommendations in this paper do not necessarily represent those of the sponsors.

References

Amoroso, S., G. Milana, K.M Rollins, C. Comina, L. Minarelli, M. R. Manuel, P. Monaco, M. Franceschini, M. Anzidei, C. Lusvardi, L. Cantore, A. Carpena, S. Casadei, F. R. Cinti, R. Civico, B. R. Cox, P. M. De Martini, G. Di Giulio, D. Di Naccio, G. Di Stefano, J. Facciorusso, D. Famiani, F. Fiorelli, D. Fontana, S. Foti, C. Madiai, V. Marangoni, D. Marchetti, S. L. Marchetti, L. Martelli, M. Mariotti, E. Muscolino, D. Pancaldi, D. Pantosti, F. Passeri, A. Pesci, G. Romeo, V. Sapia, A. Smedile, M. Stefani, G. Tarabusi, G. Teza, M. Vassallo, and F. Villani. 2017. "The first Italian blast-induced liquefaction test (Mirabello, Emilia-Romagna,Italy): description of the experiment and preliminary results." Ann Geophys 60 no, 5: S0556, https://dx.doi.org/10.4401/ag-7415

Andrus R. D., and K. H. Stokoe II. 2000. "Liquefaction resistance of soils from shear-wave velocity." J Geotech Geoenviron Eng 126, no. 11: 1015–1025, https://doi.org/10.1061/(ASCE)1090-0241(2000)126:11(1015)

Comina, C., F. Vagnon, A. Arato, and A. Antonietti 2020. "Effective Vs and Vp characterization from Surface Waves streamer data along river embankments." Journal of Applied Geophysics 183: 104221, https://doi.org/10.1016/j.jappgeo.2020.104221

Di Ludovico, M., A. Chiaradonna, E. Bilotta, A. Flora, and A. Prota. 2020. "Empirical damage and liquefaction fragility curves from 2012 Emilia earthquake data." Earthq Spectra 36 no. 2: 507-536, https://doi.org/10.1177/8755293019891713

Hossain, M. A., and R. D. Andrus. 2016. "At-rest lateral stress coefficient in sands from common field methods." J Geotech Geoenviron Eng 142 no. 12: 06016016, https://doi.org/10.1061/(ASCE)GT.1943-5606.0001560.

Idriss, I. M., and R. W. Boulanger. 2008. "Soil liquefaction during earthquakes." Report No. MNO-12. Oakland, CA: Earthquake Engineering Research Institute.

Ishihara, K. "Stability of natural deposits during earthquakes", In: 11th International Conference on Soil

Mechanics and Foundation Engineering, San Francisco, USA, 1985, Vol. 1, pp 321–376.

Iwasaki, T., F. Tatsuoka, K. Tokida, and S. Yasuda. “A practical method for assessing soil liquefaction potential based on case studies at various sites in Japan.” In: Second International Conference on Microzonation, San Francisco, 1978. pp. 885–896.

Jamiolkowski, M., D. C. F. Lo Presti, and M. Manassero. 2001. “Evaluation of relative density and shear strength of sands from cone penetration test and flat dilatometer test.” In Symposium on Soil Behaviour and Soft Ground Construction GSP 119, 201–238. Reston, VA: ASCE.

Jefferies, M., and K. Been. 2006. Soil liquefaction. A critical state approach. Hoboken, NJ: Taylor and Francis.

Marchetti, S. 1980. “In situ tests by flat dilatometer.” J Geotech Eng Div 106 no. 3: 299–321. https://doi.org/10.1061/AJGEB6.0000934

Marchetti, S. 2016. “Incorporating the Stress History Parameter KD of DMT into the Liquefaction Correlations in Clean Uncemented Sands.” J Geotech Geoenviron Eng 142 no. 2: 04015072, http://dx.doi.org/10.1061/(ASCE)GT.1943-5606.0001380

Maurer, B. W., R. A. Green, O. S. Taylor. 2015. “Moving towards an improved index for assessing liquefaction hazard: lessons from historical data” Soils Found 55 no. 4: 778–787.

Minarelli, L., S. Amoroso, R. Civico, P. M. De Martini, S. Lugli, L. Martelli, F. Molisso, K. M. Rollins, A. Salocchi, M. Stefani, and G. Cultrera. 2022. “Liquefied sites of the 2012 Emilia earthquake: a comprehensive database of the geological and geotechnical features (Quaternary alluvial Po plain, Italy).” Bulletin of Earthquake Engineering: 1-39, https://doi.org/10.1007/s10518-022-01338-7

Monaco, P., S. Amoroso, S. Marchetti, D. Marchetti, G. Totani, S. Cola, and P. Simonini. 2014. “Overconsolidation and stiffness of Venice lagoon sands and silts from SDMT and CPTU.” J Geotech Geoenviron Eng 140 no. 1: 215–227,p https://doi.org/10.1061/(ASCE)GT.1943-5606.0000965.

Park, C. B., J. Xia, R. D. Miller, 1998. Imaging dispersion curves of surface waves on multichannel record: 68th Ann Internat Mtg, Soc Explor Geophys, Expanded Abstracts: 1377-1380, https://doi.org/10.1190/1.1820161

Passeri, F., C. Comina, V. Marangoni, S. Foti, and S. Amoroso. 2018. “Geophysical tests to monitor blast-induced liquefaction, the Mirabello (NE, Italy) test site.” J Environ Eng Geoph 23, no. 3: 319-333, https://doi.org/10.2113/JEEG23.3.319

Pieri, M., and G. Groppi. “Subsurface geological structure of the Po Plain, Italy”, National Research Council of Italy, Rome, Rep. 414, 1981. (in Italian).

Seed, H. B. and I. M. Idriss. 1971. “Simplified procedure for evaluating soil liquefaction potential.” J Geotech Engrg Div 97, no. 9: 1249–1273. https://doi.org/10.1061/JSFEAQ.0001662

Robertson, P. K. (2015) ‘Guide to Cone Penetration Testing for Geotechnical Engineering’, p. 143.

Socco, L.V., Boiero, D., 2008. Improved Monte Carlo inversion of surface wave data. Geophys. Prospect. 56, 357–371.

Socco, L.V., Boiero, D., 2008. Improved Monte Carlo inversion of surface wave data. Geophys. Prospect. 56, 357–371, https://doi.org/10.1111/j.1365-2478.2007.00678.x

van Ballegooy, S. and P. Malan, 2013. “Liquefaction Vulnerability Study”. Tonkin and Taylor Ltd. Rep 52020.0200/v1.0

Tsukamoto, Y., K. Ishihara, H. Nakazawa, K. Kamada, and Y. Huang. 2002. “Resistance of partly saturated sand to liquefaction with reference to longitudinal and shear wave velocities.” Soils and foundations 6, no. 2: 93-104, https://doi.org/10.3208/sandf.42.6_93

Upadhyaya, S., R. A. Green, B. W. Maurer, A. Rodriguez-Marek, and S. Van Ballegooy. 2022. “Limitations of surface liquefaction manifestation severity index models used in conjunction with simplified stress-based triggering models.” J Geotech Geoenviron 148, no. 3: 04021194, https://doi.org/10.1061/(ASCE)GT.1943-5606.0002725

Van Ballegooy, S., P. Malan, V. Lacrosse, M. E. Jacka, M. Cubrinovski, J. D. Bray, T. D. O’Rourke, S. A. Crawford, and H. Cowan. 2014. “Assessment of liquefaction-induced land damage for residential Christchurch.” Earthq Spectra 30, no. 1: 31–55, https://doi.org/10.1193/031813EQS070M

Zhang, G., P. K. Robertson, and R. W. I. Brachman. 2002. “Estimating liquefaction induced ground settlements from CPT for level ground.” Can Geotech J 39, no. 5: 1168-1180, https://doi.org/10.1139/t02-047